

Rigid aerodynamic model and longitudinal trim optimization of A3TB flying wing configuration

Tal Sayag* and Daniella E. Raveh[†]
Technion - Israel Institute of Technology, Haifa, Israel

The report summarizes a research study on trim optimization for minimum required-thrust of the Active Aeroelastic Aircraft Testbed (A3TB) platform. The A3TB is a flying wing configuration, designed as a capstone undergraduate project, to serve as a flight vehicle for low-cost aeroelastic testing and technology implementation. One of the goals for the A3TB is to demonstrate optimized trimmed flight, in which the aircraft is flying straight-and-level while the drag (or required thrust) is minimal. Trim optimization can be potentially achieved using the A3TB eight trailing-edge control surfaces. The research study has two parts. The first part deals with aerodynamic modeling of the configuration, including the control surfaces, via a CFD code that solves the Navier-Stokes equations for the flow field about the aircraft. The second part uses the aerodynamic derivatives in a trim optimization exercise. The trim optimization goal is set as minimization of drag and control effort, and the trim equilibrium equations are used as constraints. The angle of attack and control-surface travel are the trim effectors. Control-surface travel limits are also set as constraints. Two approaches for trim-optimization were tested: The first models the drag variation as a cubic function of control surface deflections about zero trim effector values. This approach was invalidated when compared to a full CFD analysis of the supposedly optimal configuration. The other method was to compute the aerodynamic derivatives about a trimmed condition, using linear and cubic terms. With this approach, the use of the control surfaces had to be limited to small values about the trimmed condition. Trim optimization has shown a slight reduction of 1.7% in the drag, which was validated in a full CFD analysis. The study was performed considering a rigid aircraft configuration. Future studies should account for wing flexibility, and hopefully take advantage of it, in the trim optimization process.

*Undergraduate student, Faculty of Aerospace Engineering

[†]Associate Professor, Faculty of Aerospace Engineering; daniella@technion.ac.il. Senior Member AIAA.

Nomenclature

b_{ref}	= reference aerodynamic lateral dimension, [m]	q_d	= dynamic pressure, [Pa]
c_{ref}	= reference aerodynamic longitudinal dimension, [m]	S_{ref}	= reference aerodynamic area dimension, [m ²]
D	= drag force, [N]	T	= thrust force, [N]
F_x, F_y, F_z	= aerodynamic forces in body frame, [N]	U, V, W	= velocity in body frame, [m/sec]
g	= acceleration of gravity, [m/sec ²]	V	= total airspeed, [m/sec]
$I_{i,j}$	= moment of inertia around i,j plane, [Kg · m ²]	V_c	= cruise velocity, [m/sec]
\vec{k}_a	= aileron command flaps activation weight vector	V_s	= stall velocity, [m/sec]
\vec{k}_e	= elevator command flaps activation weight vector	W	= Weight [N]
\vec{k}_r	= rudder command flaps activation weight vector	\vec{w}	= control effort weight vector
\vec{k}_{th}	= throttle command flaps activation weight vector	α	= angle of attack [deg]
L	= lift force, [N]	δ_a	= collective roll command [deg]
L/D	= lift to drag ratio,	δ_e	= collective pitch command [deg]
MAC	= mean aerodynamic chord, [m]	δ_i	= i-th flap deflection [deg]
M_x, M_y, M_z	= aerodynamic moments in body frame, [N · m]	δ_r	= collective yaw command [deg]
m	= mass, [kg]	δ_{th}	= throttle command [deg]
p, q, r	= angular rate in body frame, [rad/sec]	ρ	= density of air [kg/m ³]

I. Introduction

High-altitude-long-endurance (HALE) Unmanned Aerial Vehicles (UAV) are capable of flying for a very long period of time at a very high altitude. In order to make long-endurance flight possible, new ways of reducing the required energy to operate these vehicles are being explored. One of the ways to improve the fuel efficiency of a vehicle is to reduce in weight by optimizing the structure, this affects the structural stiffness of the wing. Increased flexibility structure is more likely to experience adverse aeroelastic effects such as flutter and decreased control-surface effectiveness, which require active control measures as alternatives to stiffer aircraft.

In an effort to set up a testbed that will allow the research teams from the Faculty of Aerospace Engineering at the Technion Institute to examine static and dynamic aeroelastic phenomenon, it was decided to run a project to build an aeroelastic demonstrator. Active Aeroelastic Aircraft Testbed (A3TB) project is a 3 years undergraduate studies final project that runs since 2018 which goals are to design, build and fly a very flexible flying wing UAV with multiple control surfaces.

The current paper is a preliminary research report that it proposes is to introduce the rigid aerodynamic model that was obtained for the A3TB configuration and suggesting a method to take the advantage of this configuration redundant, under-determined, control surfaces for trim optimization while minimizing the thrust that is required for maintaining straight and level flight.

II. Mathematical Model

A. Longitudinal Trim Equations

The general longitudinal equations of motion of a free maneuvering aircraft in body coordinates, under the assumption of the rigid body, are as follows:

$$\begin{pmatrix} F_x \\ F_z \\ M_y \end{pmatrix} = \begin{pmatrix} m(\dot{U} + qW - rV) \\ m(\dot{W} + pV - qU) \\ I_{yy}\dot{q} - pr(I_{zz} - I_{xx}) - I_{xz}(r^2 - p^2) \end{pmatrix} \quad (1)$$

In order to maintain straight and level flight we should demand zero translational and rotational position rates and zero translational and rotational velocity rates. Thus, the longitudinal trim equations are reduced to the following form:

$$\begin{pmatrix} F_x \\ F_z \\ M_y \end{pmatrix} = \underline{\mathbf{0}} \quad (2)$$

Taking into consideration the aerodynamic forces, gravity and propulsion, equation (2) becomes a set of 3 equations that their solutions define the trim conditions as a function of dynamic pressure, mass, AoA, thrust and control surface deflections. One can choose the values of two of those variables and then the solution will define the other three of them. The following equations system present the full trim problem:

$$\begin{cases} F_x = T + L \sin \alpha - mg \sin \alpha - D \cos \alpha = 0 \\ F_z = mg \cos \alpha - L \cos \alpha - D \sin \alpha = 0 \\ M_y = f(\alpha, \delta_e) = 0 \end{cases} \quad (3)$$

Since we are discussing a flying wing with redundant control surfaces, we have to define an operational method for these surfaces. Conventional RC remote controller have two sticks that can transmit four basic commands: pitch (δ_e), roll (δ_a), yaw (δ_r) and throttle (δ_{th}). These commands govern the deflection of the surfaces in symmetrically or anti-symmetrically manner. Each control surface is deflected as a combination of the basic commands, each multiplied by a weighting factor that obtained from an optimization process. The deflection of each surface is then given by the following expression:

$$\delta_i = k_{e,i}\delta_e + k_{a,i}\delta_a + k_{r,i}\delta_r + k_{th,i}\delta_{th} \quad \forall i \in 1, 2, \dots, 8 \quad (4)$$

where $k_{j,i}$ are activation weights, which depend on the chosen control scheme. The expressions for lift, drag and the pitch moment due to deflection of each control surface depend on the aerodynamic model of the explored configuration. These are presented in the Test Case section. As the propulsion system is not yet defined, we can leave the thrust (T) in form of force required to maintain the trim, and later on, define it as a function of the throttle.

B. Trim Optimization Methodology

For the rigid body longitudinal trim, the optimization problem may involve multiple objectives such as drag, thrust, root-bending-moment or control effort minimization. In the current study, the optimization goal was minimization of the thrust that is required to maintain the trim, subjected to constraints on maximal (or minimal) allowable angle of attack (AoA) and control-surface deflections, maximal control effort, and satisfaction of the trim equations as formulated in Eq(3).

1. Thrust Minimization

A parameter that can be critical for the performance of the aircraft, such as flight duration and maneuverability is the required power from the propulsion system. Higher efficiency is correlated with lower required power. As the engine model is still undefined, the power will be presented by the required thrust for maintaining the desired maneuver. For multiple control-surface configuration, the travel of flaps as a function of elevator command (δ_e) can be defined in many ways. In order to preserve travel margin of the flaps as a function of another command such as aileron, the weighted control effort will also be minimized. The multiple objective optimization problems for thrust and control effort minimization can be defined by:

Minimize	T $100 \sqrt{\frac{1}{8} \sum_{i=1}^8 \left(w_i \frac{\delta_i}{\delta_{i_{max}}} \right)^2}$	Thrust	
		Weighted control effort limit	
Subject to	$\alpha_{min} \leq \alpha \leq \alpha_{max}$	AoA Limits	(5)
	$-\delta_{i_{max}} \leq \delta_i \leq \delta_{i_{max}}, \forall i \in 1, 2, \dots, 8$	Surfaces deflection limits	
	Eq.(3)	Satisfy trim equations	

The current optimization problem was solved by a multi-objective genetic algorithm using the Matlab program (function *gamultiobj*). During the optimization process, the trim equations are solved by Matlab embedded numerical equation solver.

III. Test Case

A. Geometric Model

The aircraft investigated in this study has an airframe similar to the Body Freedom Flutter demonstrator developed by LM Aero and AFRL. The vehicle is a high aspect ratio flying wing which will be used as the main platform of A3TB undergraduate students' final design project. Figure 1 shows the general geometry of the demonstrator and Table 1 has the main structural parameters.

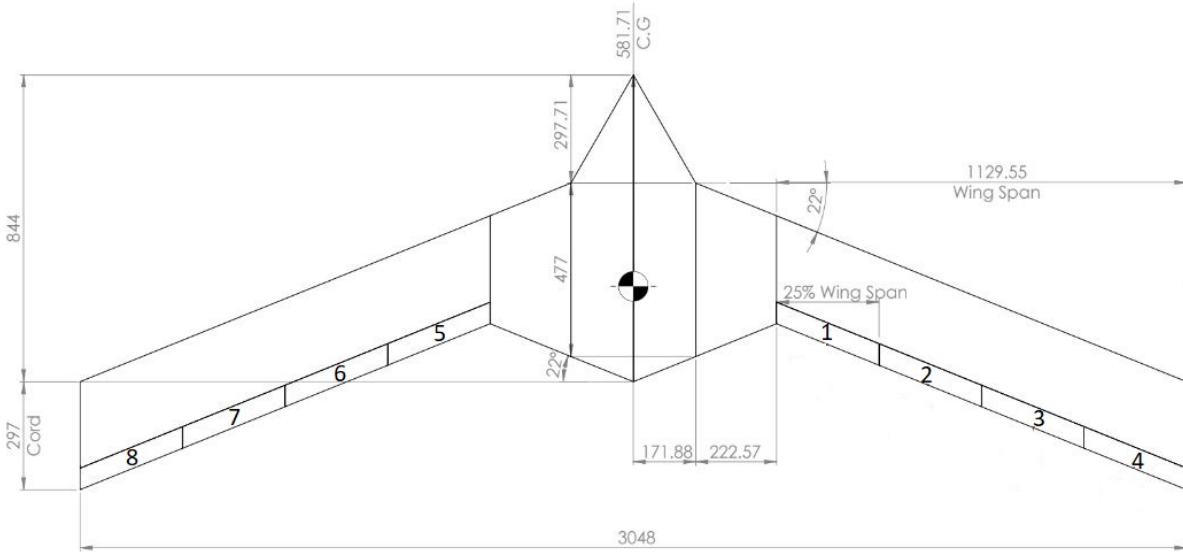


Fig. 1 A3TB demonstrator general geometry

Parameter	value
Mass [kg]	8
Wing surface area [m^2]	1.07
Wing span [m]	3.048
Wing chord [m]	0.297
Mean aerodynamic chord (MAC) [m]	0.395
Wing swept angle [deg]	22
Aspect ratio	8.4
Airfoil	NACA0012

Table 1 A3TB Structural parameters

The A3TB demonstrator has a total of eight control surfaces; four surfaces on each wing. The current study assumes that the whole configuration (body and wings) behave as a rigid body. Both the wing and the body have a symmetrical

NACA 0012 airfoil.

B. Aerodynamic Model

A complete aerodynamic analysis was conducted using the EZNSS Computational Fluid Dynamics (CFD) software. CFD mesh was generated based on the CAD model of the vehicle for viscous turbulent analysis. The full configuration viscous mesh has dimensions of 545, 345, 149 in the chordwise, spanwise and perpendicular directions respectively. The grid extends 110 chords to the far field. Forces and moments were computed by the CFD analysis. The pressure distribution at sections along the span were computed based on the CFD pressure distribution using dedicated Matlab routines.

1. Stability and control derivatives

Figure 2 illustrates the coordinate system used in the analyses. Table 2 presents the reference dimensions that were used for normalization of the aerodynamic coefficients. The moment coefficients were computed about x_{ref} . Figure 3 shows the force and moment coefficients as a function of AoA in the flow coordinate system. An additional process of curve fitting was performed in order to obtain the stability derivatives. Table 3 summarized all of the longitudinal aerodynamic derivatives and parameters.

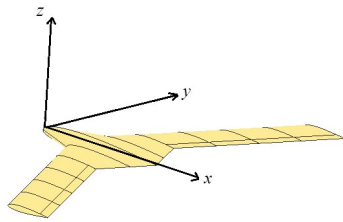


Fig. 2 Aerodynamic model coordinate system

Parameter	value
$S_{ref}[m^2]$	1.07
$c_{ref}[m]$	0.3
$b_{ref}[m]$	3
$x_{ref}[m]$	0.583

Table 2 A3TB longitudinal aerodynamic parameters

Figure 4 shows the forces and moments due to flaps deflection, as computed by CFD analysis. Table 4 summarizes the resulting aerodynamic coefficients, under the assumption of symmetrical influence of flaps on drag and lift. Positive deflection is defined as tilting the surface downwards, resulting in pitch down moment about the CG.

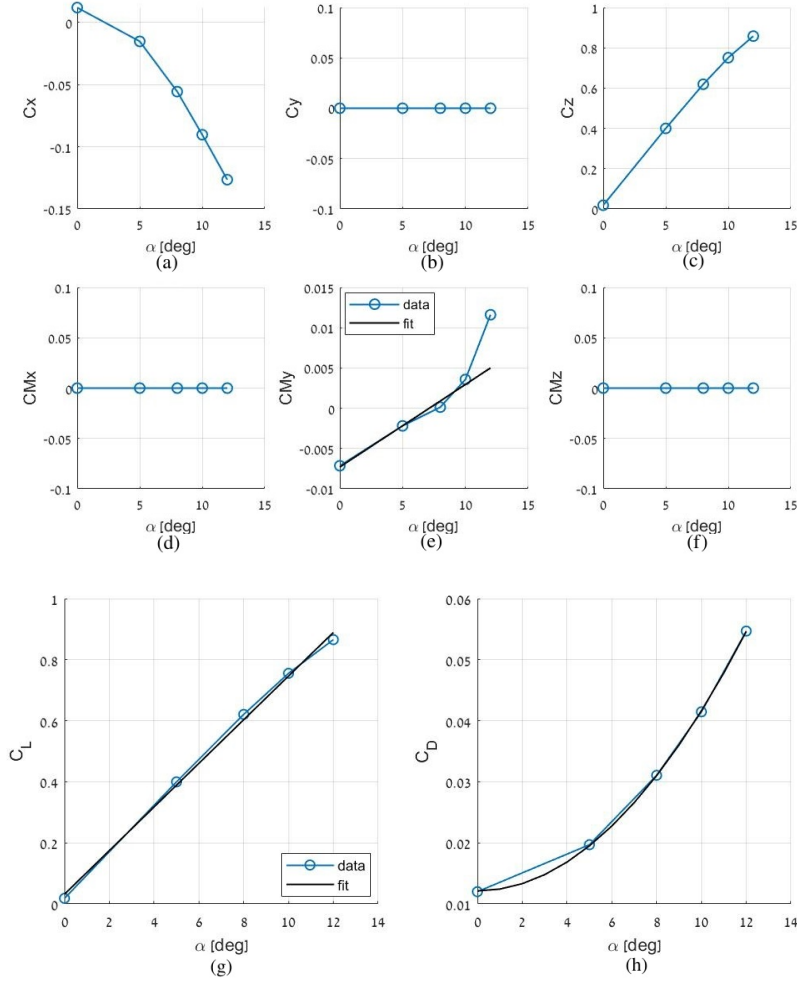


Fig. 3 Force and Moment coefficients as function of AoA

2. Linear longitudinal aerodynamic model

Under the assumptions of the linear aerodynamic model and rigid body, the longitudinal aerodynamic forces and moment for level flight (under elevator command only) are given by:

$$\begin{aligned}
 L &= q_d S_{ref} (C_{L_\alpha} \alpha + \sum_{i=1}^8 C_{L_{\delta_i}} (\delta_e k_{i,e})) \\
 D &= q_d S_{ref} (C_{D_0} + C_{D_{\alpha^2}} \alpha^2 + \sum_{i=1}^8 C_{D_{\delta_i^2}} (\delta_e k_{i,e})^2) \\
 M_y &= q_d c S_{ref} (C_{M_\alpha} \alpha + \sum_{i=1}^8 C_{M_{\delta_i}} (\delta_e k_{i,e}))
 \end{aligned} \tag{6}$$

Where $q_d = \frac{1}{2} \rho V_\infty^2$ is the dynamic pressure. It is noted that the drag force is dependent on the AoA squared and on the deflection of each control surface squared. This is in accordance with the fit for the AoA and control surfaces shown in Figure 3 and 4, respectively. The assumption of linearity is valid up to AoA of 10 deg as shown in Figure 3e. The

Parameter	value
C_{L_0}	0.032
$C_{L_\alpha} [\frac{1}{rad}]$	4.1
C_{M_0}	-0.0073
$C_{M_\alpha} [\frac{1}{rad}]$	0.0587
$C_{D_0} [\frac{1}{rad}]$	0.0121
$C_{D_{\alpha^2}} [\frac{1}{rad^2}]$	0.9686

Flap	$C_{L_{\delta_i}}$	$C_{D_{\delta_i^2}}$	$C_{L_{\delta_i}}$	$C_{M_{\delta_i}}$	$C_{N_{\delta_i}}$
1 (5)	0.1809	0.0197	+(-)0.0283	-0.0086	-(+)0.0029
2 (6)	0.1617	0.0208	+(-)0.0395	-0.0550	-(+)0.0046
3 (7)	0.1228	0.0186	+(-)0.0398	-0.0791	-(+)0.0054
4 (8)	0.1049	0.021	+(-)0.0414	-0.1010	-(+)0.0083

Table 4 A3TB flaps deflection aerodynamic parameters
 $[\frac{1}{rad}]$

Notes:

- 1) C_{M_α} is positive due to arbitrary reference point (not CG).
- 2) C_{L_0} and C_{M_0} exist due to an undesired defect in the CAD model for which the airfoil was not exactly symmetric.

Table 3 A3TB longitudinal aerodynamic parameters

resulted derivatives around zero AoA and zero flaps deflection were substituted into Eq(3) in order to solve the trim equations during the optimization process.

3. Stall performance

The stall AoA and maximal lift coefficient were determined from CFD analyses at several AoA values. Figure 5 shows the lift coefficient as a function of the AoA. As can be seen in Figure 5 the lift coefficient is linear at a range of $\alpha \in [0, 12][deg]$ and becomes saturated at 14 degrees. It is noted that at $\alpha = 14[deg]$ the CFD run did not converge. Thus, we chose to fix the maximum angle of attack at $12[deg]$ and $C_{L_{Max}} = 0.86$.

C. Control Schemes

1. Conventional

The conventional trim approach for the multi-flaps flying wing is based on using only the two outer flaps to execute aileron commands, while for elevator command, all flaps are deflected together as a single large trailing-edge flap.

2. Optimal

Using an optimization process to determine the deflection pattern that will meet the optimization objectives and constraints. The solution of the optimization problem fixes a gearing ratio between all flaps. In the current study, the optimization will determine the elevator gearing ratio.

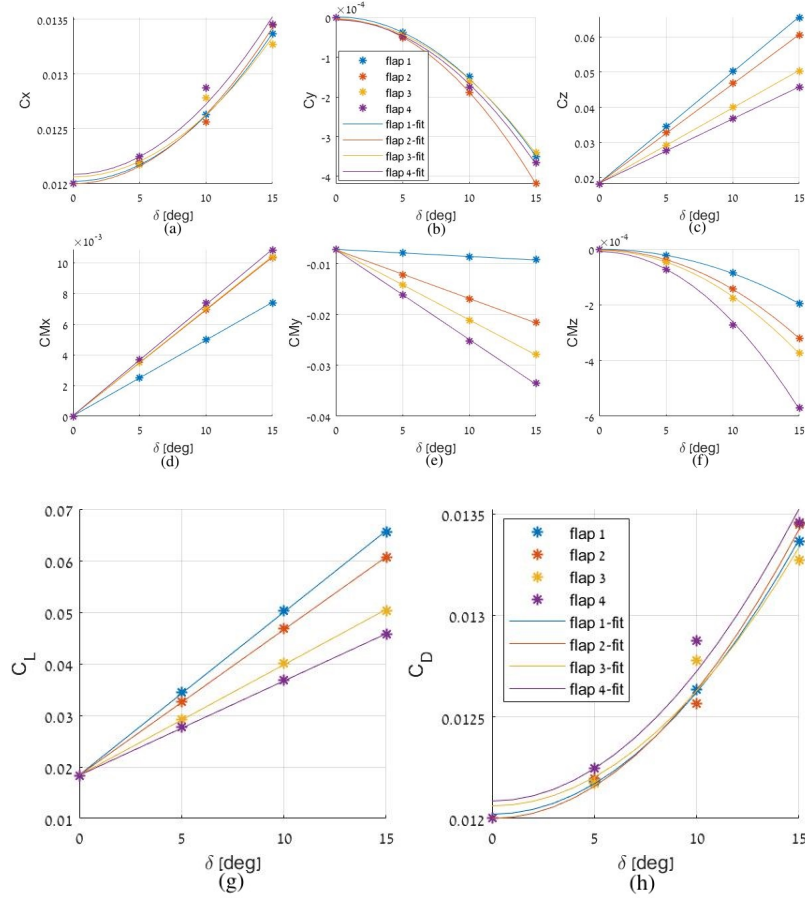


Fig. 4 Force and Moment coefficients as function of flap deflections

D. CG location

Our main criterion for determining the desired center of gravity location along the x-axis is the required control effort (flaps deflection) for trimming the aircraft using the conventional control scheme. Thus, we made an analysis of elevator position as a function of CG location for maintaining trim at stall speed. Figure 6 shows the obtained results. A3TB configuration flaps travel are limited to $\pm 15[deg]$, in order to ensure control ability for maneuver beyond the trim position. We chose to locate the CG at $x = 0.55[m]$ which yields approximately 8%[MAC] of stability margin. For this CG location the flaps are deflected at $9[deg]$ at trim at the stall speed.

E. Flight Conditions

Trim optimization is performed for cruise flight, which makes the majority of the flight time. To determine the cruise speed of the flying wing, first, the stall speed for different load factor values was calculated:

$$V_s = \sqrt{\frac{2nW}{\rho S_{ref} C_{L_{max}}}} \quad (7)$$

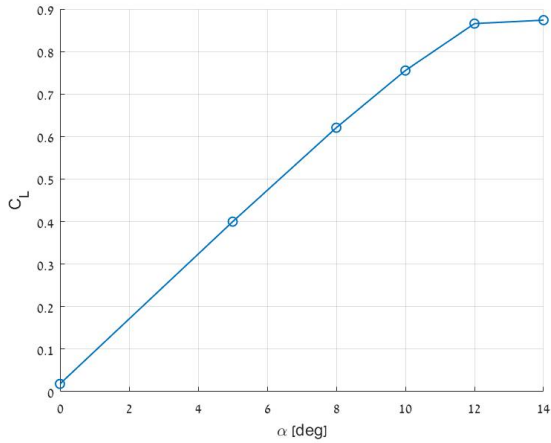


Fig. 5 Lift as function of AoA

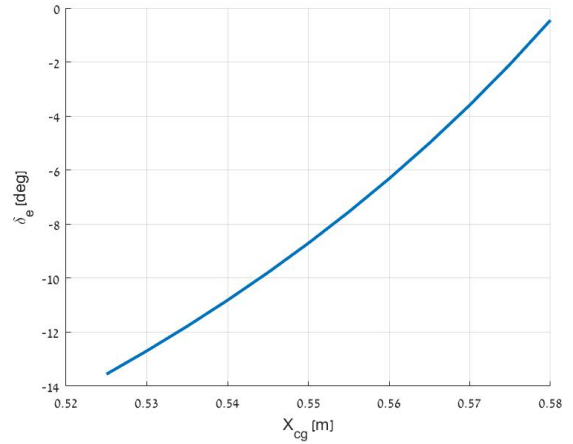


Fig. 6 Flaps position for trim at $C_{L_{max}}$ using conventional control at different CG location

from which, the stall speed for straight and level flight was found to be 25 knots. Without any other requirements, it is common to determine the cruise speed as the speed for which the lift-to-drag (L/D) ratio is maximal. Figure 7 presents the $\frac{L}{D}$ ratio as a function of velocity for conventional control scheme at trim. The maxima is obtained at flow velocity around 35 knots. This speed which is 140% the stall speed will be referred to as the cruise speed, V_c . In order to perform the trim optimization at non-optimal $\frac{L}{D}$ operating point, the conditions for trim optimization are chosen to be at standard sea level condition, $\rho = 1.225[\frac{kg}{m^3}]$ and $V = 40[kt]$.

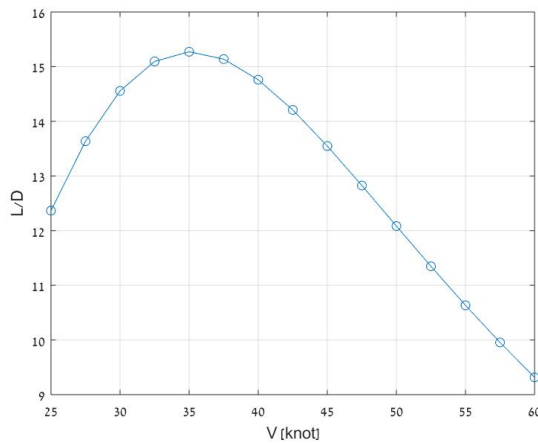


Fig. 7 Lift-to-drag ratio as function of velocity using conventional control scheme trimmed aircraft

IV. Optimization Results

A. Trim using conventional control scheme

In the conventional approach for trimming an aircraft, trim is obtained via the angle of attack and an elevator, which, in our case, translates to deploying all flaps together. Using a conventional control scheme Eq(3) system has a unique solution for the trim problem at any given airspeed. Figure 8 shows the thrust that is required to maintain trim at the flight envelope velocity range. The thrust required to maintain the trim at $V = 40[kt]$ is $T = 5.30[N]$, the required AoA is $\alpha = 4.50[deg]$ and all flaps deflect upward at $3.95[deg]$. Figure 9 shows these results visually.

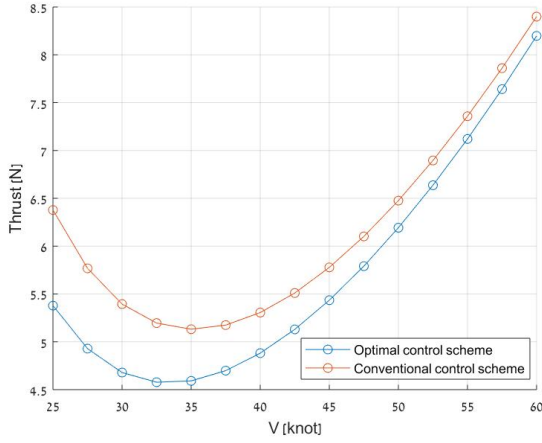


Fig. 8 Thrust as function of velocity using conventional and optimal control schemes

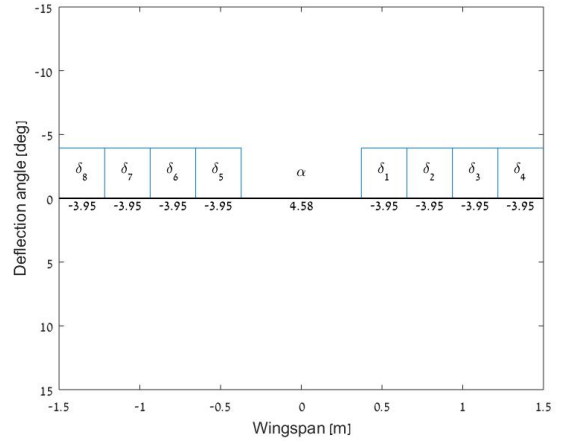


Fig. 9 AoA and flaps deflection at $V = 40[kt]$ using conventional control scheme

B. Trim using optimal control scheme

In order to obtain the optimal gearing ratio to maintain trim with minimal thrust and control effort, we solve the optimization problem as described in Eq(5), subject to:

$$\begin{aligned}
 -4 \leq \alpha \leq 12 & & \text{AoA Limits [deg]} \\
 -15 \leq \delta_i \leq 15, \forall i \in 1, 2, \dots, 8 & & \text{Surfaces deflection limits [deg]} \\
 \vec{w} = [0, 0.25, 0.5, 1, 0, 0.25, 0.5, 1] & & \text{Control effort weights} \\
 \delta_i = \delta_{i+4}, \forall i \in 1, 2, 3, 4 & & \text{Symmetrical flaps deflection condition}
 \end{aligned} \tag{8}$$

We intended to perform a multi-objective optimization in order to minimize: 1) thrust 2) control effort that are required for trim. We have four optimization variables (activation weights, \vec{k}_e) and another three parameters, AoA α , collective pitch command δ_e , and thrust T that are derived from them. Solving the following under-determined

system results in infinite number of valid solutions. A Pareto frontier that represents the trade-off between thrust and control-effort optimal solutions is shown in Figure 10.

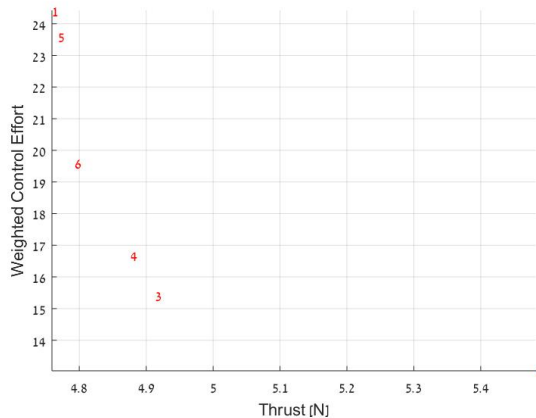


Fig. 10 Pareto frontier: Thrust vs. wighted control effort

Under demand for low control effort, we chose case 4 from the Pareto frontier. The yielded activation weights that obtained from solving this optimization problem are:

$$\vec{k}_e = [0.80, -0.50, -1.00, -0.48, 0.80, -0.50, -1.00, -0.48] \quad (9)$$

The thrust required to maintain the trim using the optimal gearing ratio at $V = 40[kt]$ is $T = 4.88[N]$, the required AoA is $\alpha = 3.84[deg]$ and the collective pitch command δ_e is $6.58[deg]$. Figure 11 shows the control surfaces deflection pattern of the optimal solution. Figure 8 shows the thrust required for trim for the optimal deflection pattern, compared to that of conventional trim. Although optimization was carried out at single velocity, the improvement is reflected at all velocity range.

These results present a reduction of 8 percent in the required thrust for maintaining trim flight at $V = 40[kt]$. This is certainly a considerable improvement in efficiency.

V. Results Validation

In order to check the validity of the findings, we run CFD analyses that represents the two control schemes (both conventional and optimal). We expect to find that the approximate aerodynamic model that we construct for the A3TB configuration accurately capture the actual aerodynamic forces and moments. Thus, we expect that both these runs will indicate a trimmed aircraft. Furthermore, we expected that a comparison of the drag will indicate that the optimal control scheme indeed results in lowered drag.

Table 5 summarizes the differences between the optimization results using the linear model and as computed by the

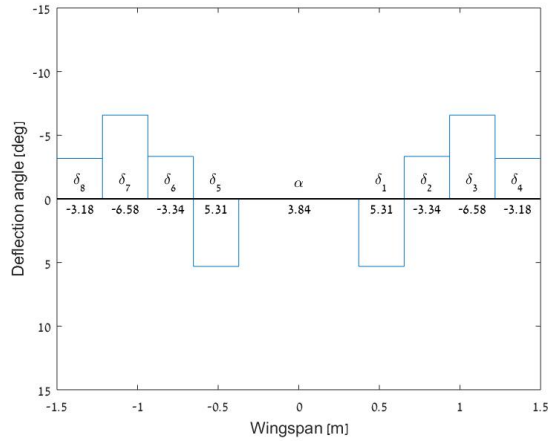


Fig. 11 AoA and flaps deflection at $V = 40[kt]$ using optimal control scheme

CFD analyses. In the CFD analyses of both the conventional and the optimal configurations the trim conditions (of C_L and C_M) are not met exactly. Moreover, there is a significant mismatch between the estimated drag values using the aerodynamic model and those calculated accurately using CFD.

Parameter	Conventional control		Optimal control	
	Linear Model	CFD	Linear Model	CFD
Flaps weights (one side)	[1 , 1 , 1 , 1]		[0.80 , -0.50 , -1.00 , -0.48]	
Angle of attack [deg]	4.58		3.83	
Collective elevator command [deg]	-3.95		6.58	
C_L	0.281	0.285	0.280	0.287
C_D (counts)	191	164	176	164
C_M	0	-0.013	0	-0.020

Table 5 Linear model vs. CFD result comparison

The CFD analyses of the optimal control scheme did not indicate any drag reduction as compared with the conventional trim. This indicates that the aerodynamic model used for trim optimization is either not accurate enough or even non-valid.

VI. Detailed local aerodynamic model

In order to verify that the observed differences were due to the lack of suitability of the aerodynamic model, a new model was derived based on wider CFD analyses. The new model gives higher accuracy in AoA range of two and half up to eight degrees, which is the expected range for the optimal trim. The control surfaces influence was calculated at angle of attack of five degrees and takes into consideration the asymmetric influence of positive or negative deflection.

The dependence of lift, drag, and pitch moment on the angle of attack and each flap deflection was fitted using quadratic equations, as shown in Figure 12.

In that way the forces and moment of the longitudinal plane obtained using the following equations:

$$\begin{aligned}
 L &= q_d S_{ref} \{ C_{L_\alpha} \alpha + C_{L_{\alpha^2}} \alpha^2 + \sum_{i=1}^8 [C_{L_{\delta_i}} (\delta_e k_{i,e}) + C_{L_{\delta_i^2}} (\delta_e k_{i,e})^2] \} \\
 D &= q_d S_{ref} \{ C_{D_\alpha} \alpha + C_{D_{\alpha^2}} \alpha^2 + \sum_{i=1}^8 [C_{D_{\delta_i}} (\delta_e k_{i,e}) + C_{D_{\delta_i^2}} (\delta_e k_{i,e})^2] \} \\
 M_y &= q_d S_{ref} \{ C_{M_\alpha} \alpha + C_{M_{\alpha^2}} \alpha^2 + \sum_{i=1}^8 [C_{M_{\delta_i}} (\delta_e k_{i,e}) + C_{M_{\delta_i^2}} (\delta_e k_{i,e})^2] \}
 \end{aligned} \tag{10}$$

We implemented these expressions in the same optimization problem as given in equation (5), in order to find out the optimal control surfaces deflection for minimum required thrust. The thrust required to maintain the trim using the optimal gearing ratio with the new model at $V = 40[kt]$ is $T = 4.17[N]$, the required AoA is $\alpha = 4.0[deg]$. Figure 13 shows the control surfaces deflection pattern of the optimal solution.

As before, we run CFD analysis that represents the new optimal control schemes in order to validate the new results. Table 6 summarizes the differences between the optimization results using the new quadratic model and as computed by the CFD analyses. The results of the conventional control were calculated again too, with the new model. A reduction of 5 counts gained using the analytical model, which is 3.2% of the total drag. In the CFD analyses of both the conventional and the optimal configurations the trim conditions (of C_L and C_M) are not met exactly, but the moment coefficients are closer to zero than those found using the previous model.

Parameter	Conventional control		Optimal control	
	Quadratic Model	CFD	Quadratic Model	CFD
Flaps weights (one side)	[1 , 1 , 1 , 1]		[0.07 , -0.07 , -0.55 , -1.00]	
Angle of attack [deg]	4.51		4.00	
Collective elevator command [deg]	-3.69		6.5	
C_L	0.281	0.287	0.281	0.289
C_D (counts)	155	164	150	161
C_M	0	-0.002	0	-0.002

Table 6 Linear model vs. CFD result comparison

The CFD analyses of the optimal control scheme indicate a drag reduction of only 3 counts which is 1.7% as compared with the conventional trim. This indicates that the new quadratic aero model used for this trim optimization match the results from the CFD much more than the model that was introduced before. Thus, we approved that improving the accuracy of the aerodynamic model can lead to better performance of the optimization process in prediction of the optimal flap deflection of minimum drag.

VII. Conclusions

The current paper detailed the main actions that taken in order to establish a valid and representative aerodynamic model and performing optimization process in order to reduce required thrust for trimming A3TB flying-wing configuration. CFD has been widely used for aerodynamic analysis from which the linear aerodynamic and later the local quadratic model was constructed.

Using the obtained model to perform the multi-objective optimization yield a Pareto frontier that shows that it is theoretically possible to reduce the required thrust using differential flaps deflection along the wingspan. Control effort was included in the optimization objectives in order to ensure that sufficient control remains available for maneuvering. A significant improvement of 8% was introduced using theoretical optimization based on the simple linear model.

Validation of results using CFD was failed. As a result, it can not be concluded that the linear aerodynamic model is consistent with the results produced by the CFD. The gaps presented in these results can be due to a number of different reasons: 1) Physical couplings between the flaps deflection and the angle of attack that were not taken into account. 2) Inappropriate modeling of the CFD grid, and flaps deflection. 3) Inconsideration asymmetrical effect of tilting the flaps up or down.

In order to confirm that drag reduction can be achieved using the proposed optimization process, A new local detailed quadratic aerodynamic model was introduced. Reduction of 1.7% of the total drag was obtained using the differential control surfaces deflection.

A follow-up study is required after renovating the necessary corrections to the possible faults that have been raised. More detailed global aerodynamic model is needed in order to fully exploit the ability of drag reduction. It is also recommended to choose operating point with more induced drag (at slower velocities), in order to ensure better optimal solution.

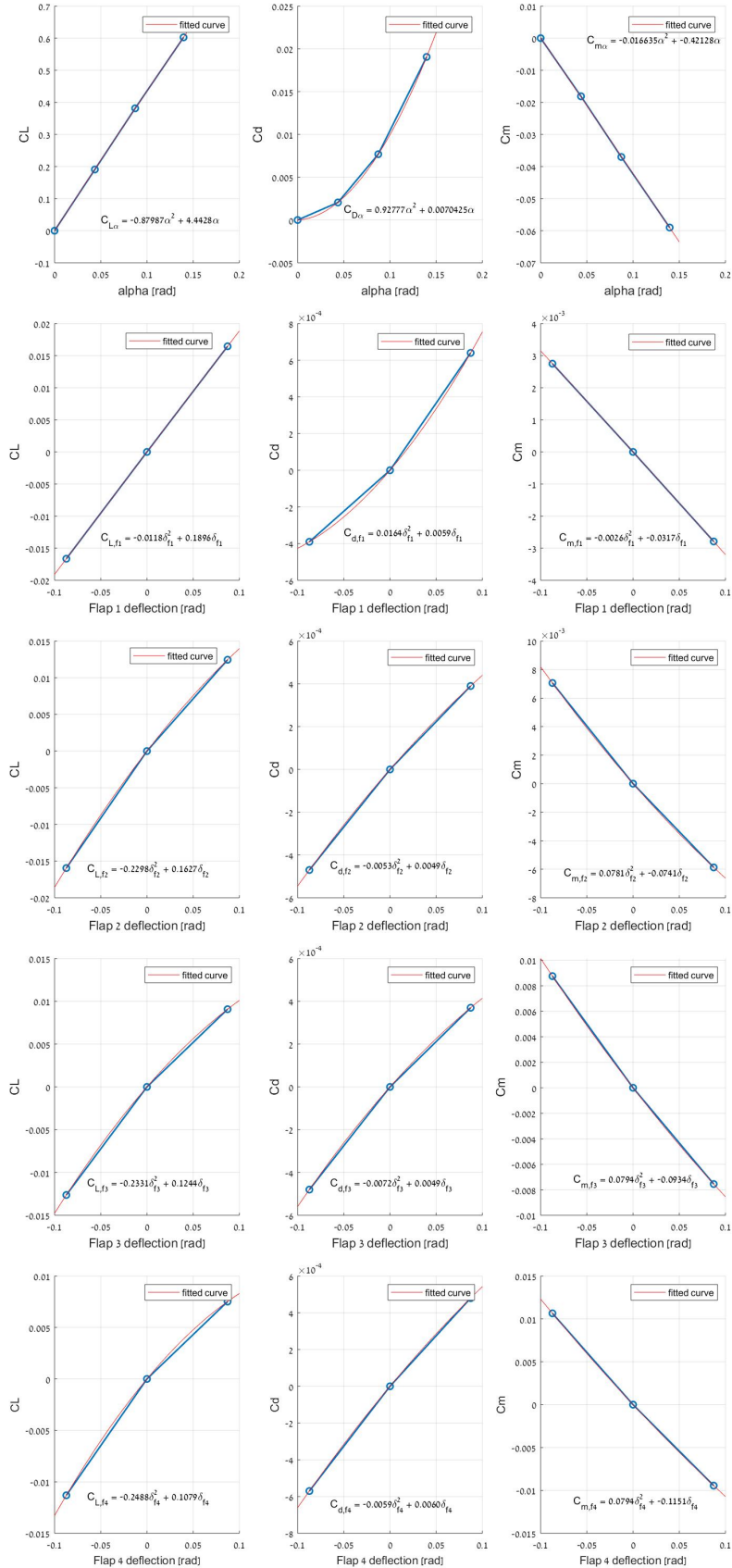


Fig. 12 Detailed local aerodynamic model around $\alpha = 5[deg]$. Data points from CFD and fitted curves

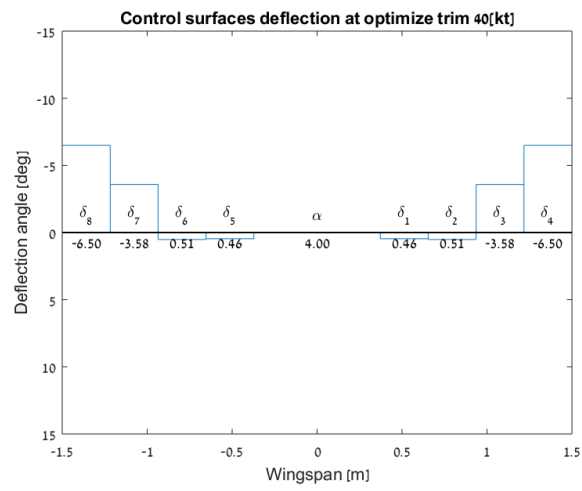


Fig. 13 AoA and flaps deflection at $V = 40[kt]$ using optimal control scheme derived from the new model